Journal of Surface Engineered Materials and Advanced Technology, 2012, 2, 149-157
http://dx.doi.org/10.4236/jsemat.2012.23024 Published Online July 2012 (http://www.SciRP.org/journal/jsemat)

Effect of Filler Content and Alkalization on Mechanical and Erosion Wear Behavior of CBPD Filled Bamboo Fiber Composites

Anu Gupta[1], Ajit Kumar[1], Amar Patnaik[2*], Sandhyarani Biswas[2]

[1]School of Engineering and Technology, Indira Gandhi National Open University, New Delhi, India; [2]Mechanical Engineering Department, National Institute of Technology, Hamirpur, India.
Email: [*]amar_mech@sify.com

Received September 30th, 2011; revised October 13th, 2011; accepted November 8th, 2011

ABSTRACT

In this study the mechanical and erosion wear behavior of bamboo fiber reinforce epoxy composites filled with Cement By-Pass Dust (CBPD) were studied. The effect of CBPD content and alkalization on the various properties of these composites was also investigated. Taguchi's orthogonal arrays are used for analysis of experiential results. It identifies significant control factors influencing the erosion wear and also outlines significant interaction effects. Analysis of variance (ANOVA) test has also been performed on the measured data to find the most significant factors affecting erosion rate. Finally, eroded surfaces of both untreated and alkali treated bamboo fiber reinforced composites were characterized using SEM.

Keywords: Composites; Bamboo Fiber; Mechanical Property; Erosion Wear; CBPD

1. Introduction

Over the last decade there has been renewed interest in the use of natural fibers to replace synthetic fibers in composite applications. Compared with conventional fibers natural fibers have many advantages like renewable, environmental friendly, low cost, lightweight, high specific mechanical performance. Among various natural fibers bamboo is one the most potential reinforcement for fiber reinforced polymer composites. Bamboo has numerous advantages over other natural fibers such as its availability, excellent mechanical properties in comparison with its weight due to longitudinally aligned fibers, one of the fastest renewable plants etc. However, being hydrophilic, natural fibres need to be chemically treated first to make them more compatible with hydrophobic polymers. Several researchers have reported improvement in properties of natural fibers when alkalized at different NaOH concePnotlryamtioenrs [1-4] generated a wide interest in the engineering domain, including their tribological applications [5], in view of their good strength and low density as compared to monolithic metal alloys. Being light-weight, they are the most suitable materials for weight sensitive applications, but their high cost becomes a limiting factor for commercial applications. However, it has been observed that by incorporating filler particles into the fiber reinforced composites the performance of composites can be improved [6-12]. Cement By-Pass Dust (CBPD) is a by-product of cement manufacturing. It is a fine powdery material similar to Portland cement in appearance. It is generated during the calcining process in the kiln. As the raw materials are heated in the kiln, dust particles are produced and then carried out with the exhaust gases at the upper end of the kiln. These gases are then cooled and the accompanying dust particles are captured by efficient dust collection systems. Lime (CaO) constitutes about 40% of CBPD composition. Other compounds include SiO_2, Al_2O_3, Fe_2O_3, K_2O, Na_2O, etc.

To this end, the present research work is undertaken to study the mechanical and erosion wear behavior of bamboo fiber reinforce epoxy composites filled with Cement By-Pass Dust (CBPD) were studied. The effect of CBPD content and alkalization on the various properties of these composites was also investigated. Taguchi's orthogonal arrays are used for analysis of experiential results. And analysis of variance (ANOVA) test has also been performed on the measured data to find the most significant factors affecting erosion rate.

2. Experimental Details

2.1. Composite Fabrication

Epoxy LY-556 and the hardener (HY951) supplied by

[*]Corresponding author.

Ciba Geigy India Ltd. and the bi-directional bamboo fibers, collected from local sources have been taken as raw materials for composite fabrication. Each ply of roving bi-directional bamboo mats is of dimension 150 × 150 mm^2. Composite slabs are made by reinforcing bi-directional bamboo mats in epoxy resin using simple hand lay-up technique followed by light compression molding technique. Composites of three different compositions (with 0 wt%, 10 wt% and 20 wt% of CBPD filling) are made with constant bamboo fiber loading of 40 wt% for all the composite samples. For treatment of bamboo fibers, bi-directional bamboo fibers are soaked in 20% caustic soda solution at ambient temperature, maintaining a liquor ratio of 15:1. The fibers are kept immersed in the alkali solution for 1 hour. Then the fibers are copiously washed with distilled water to remove any traces of alkali sticking to the fiber surface and subsequently neutralized with 2% sulfuric acid solution. The neutrality is checked with litmus paper. Fibers are finally dried in a hot air oven at 100˚C. Untreated fibers were also dried in an oven. The castings are put under load for about 24 hours for proper curing at room temperature. After the curing process, test samples are cut to the required sizes as per individual test requirement.

2.2. Measurements

2.2.1. Physical and Mechanical Tests

The theoretical density of composite materials is obtained as per the equations given by Agarwal and Broutman [13]. However, the actual density of the composites is determined experimentally by simple water immersion technique. Tensile tests were performed on Instron 1195. The tests were carried out in accordance with ASTM D 3039-76. The dimensions of the specimen were 150 mm × 10 mm × 4 mm. Composite samples were tested at a crosshead speed of 10 mm/min. Flexural tests (three point bend test) were conducted on all the composite samples using Instron 1195. The dimension of the specimen is 60 mm × 10 mm × 4 mm. A thickness of 4 mm is maintained for all composite samples. Span length of 40 mm and the cross head speed of 10 mm/min are maintained. Short beam shear test is carried out on composite samples to determine the inter-laminar shear strength (ILSS). Impact tests were done as per ASTM D 256 using an impact tester. The pendulum impact testing machine ascertains the notch impact strength of the material by shattering the V notched specimen with a pendulum hammer, measuring the spent energy, and relating it to the cross section of the specimen.

2.2.2. Erosion Test

Erosion tests were performed on an erosion test rig as per ASTM G76. The rig consists of an air compressor, a particle feeder, an air particle mixing and accelerating chamber. Dry compressed air is mixed with the particles, which are fed at a constant rate from a conveyor belt type feeder in to the mixing chamber and then accelerated by passing the mixture through a tungsten carbide (WC) converging nozzle of 3 mm diameter. These accelerated particles hit the specimen, and the specimen can be held at various angles using an adjustable sample holder. The feed rate of the particles can be controlled by monitoring the distance between the particle feeding hopper and the belt drive (carrying these particles to mixing chamber). The impact velocity of the particles can be varied by varying the pressure of the compressed air and can be measured using a rotating disc method [14]. In the present study pyramidal shaped dry silica sand of different particle sizes (125 μm to 355 μm) were used as erodent. A standard test procedure was employed for each erosion test. The samples were cleaned in acetone, dried and weighed to an accuracy of 1×10^{-5} g using an electronic balance, eroded in the test rig for 5 min and then weighed again to determine the weight loss. The ratio of this weight loss to the weight of the eroding particles causing the loss (*i.e.* testing time × particle feed rate) is then computed as the dimensionless incremental erosion rate. This procedure is repeated till the erosion rate attains a constant steady-state value. Finally the SEM micrographs of treated and untreated fiber composite surfaces were taken using a scanning electron microscope Model JEOL JSM-6480LV.

2.3. Experimental Design

A designed experiment is an approach to systematically varying the controllable input factors and observing the effect these factors have on the output product parameters. The Taguchi's approach provides the designer with a systematic and efficient approach for conducting experimentation to determine optimum settings of design parameters for performance and cost. The steps included in the Taguchi parameter design are: selecting the proper orthogonal array (OA) according to the numbers of controllable factors (parameters); running experiments based on the OA; analyzing data; identifying the optimum condition; and conducting confirmation runs with the optimal levels of all the parameters. As applying Taguchi parameter design requires the identification of factors affecting targeted quality characteristics, relevant literature must be reviewed to screen the most important among a number of factors or conditions affecting erosion rate of composites. Five parameters, viz. impact velocity, fiber loading, stand-off distance, impingement angle, and erodent size, each at three levels, are considered in this study in accordance with L27 (313) orthogonal array design. The operating parameters and their levels con-

sidered for erosion tests are listed out in **Table 1**.

The plan of the experiments is as follows: the first column was assigned to factor A, the second column to factor B, the fifth column to factor C, the ninth column to factor D and tenth column to factor E, the third and fourth column are assigned to (A × B)1 and (A × B)2 respectively, to estimate interaction between factor A and factor B, the sixth and seventh column are assigned to (B × C)1 and (B × C)2 respectively, to estimate interaction between the factor B and factor C, the eighth and eleventh column are assigned to (A × C)1 and (A × C)2 respectively, to estimate interaction between the factor A and factor C. The remaining columns are assigned to error column.

3. Results and Discussion

3.1. Effect of Filler Content and Mechanical Properties of Composites

The experimental density includes all the solid material and the pores within the fibers and is always less than the theoretical density, which excludes all the pores and lumen due to the buoyancy effect caused by the trapped air. Lower experimental density indicates higher porosity as pores have been found to reduce the density of materials. The theoretical and measured densities along with the corresponding volume fractions of voids are presented in **Figure 1(a)**. The variation of void content with the CBPD content for both treated and untreated bamboo fiber based composites is shown in **Figure 1(a)**. It is observed from the figure that the void fraction of untreated composites increases with increase in filler content.

However it shows a significant change in case of alkalized bamboo fiber based composites where the void fraction decreases with increase in filler content.

The variation of micro-hardness values of composites with CBPD content is shown in **Figure 1(b)**. The test results show that with the presence of CBPD, hardness (Hv) value of the untreated and treated bamboo epoxy composites is improved and this improvement is a function of the CBPD content. Similar trend is also observed by previous investigators [15-17].

Table 1. Parameter settings.

Control factor	Level			
	I	II	III	Units
A: Velocity of impact	45	55	65	m/sec
B: Filler content	0	10	20	%
C: Impingement angle	30	60	90	degree
D: Stand-off distance	65	75	85	mm
E: Erodent size	125	250	350	µm

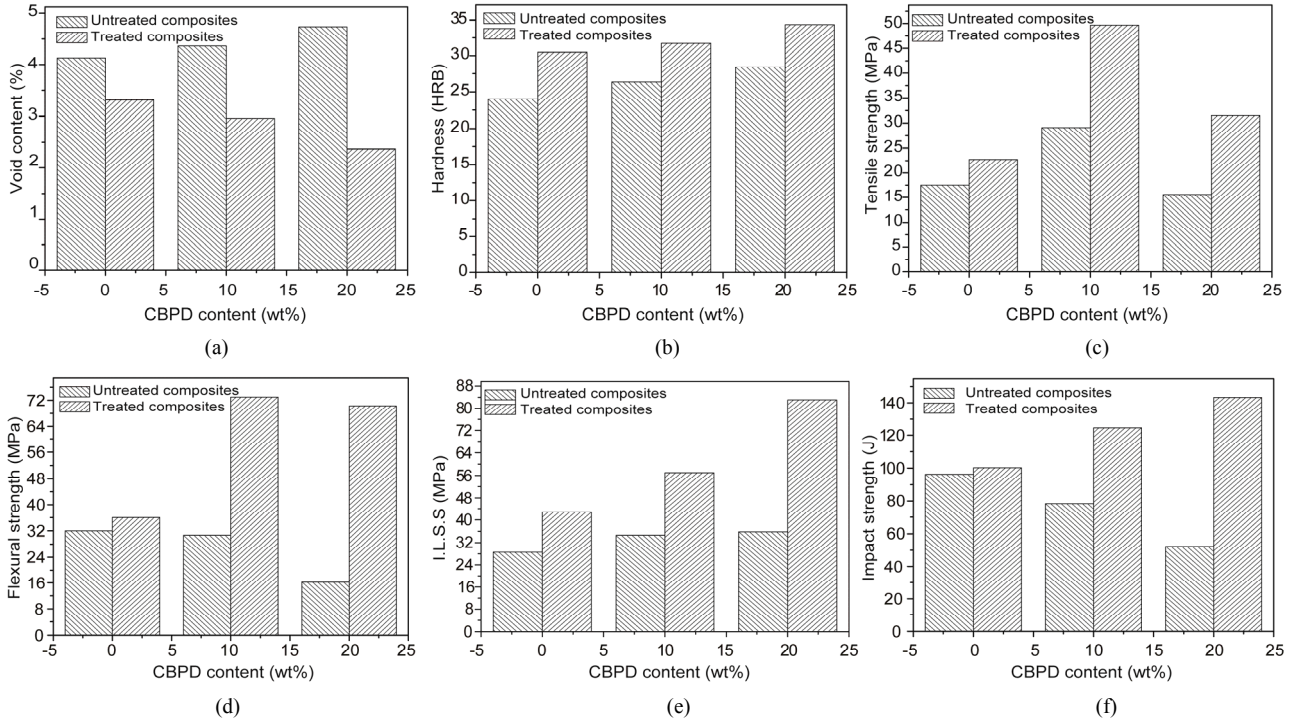

Figure 1. (a) Void content of bamboo fiber based composites; (b) Micro-hardness of bamboo fiber based composites; (c) Tensile strength of bamboo fiber based composites; (d) Flexural strength of bamboo fiber based composites; (e) ILSS of bamboo fiber based composites; (f) Impact strength of bamboo fiber based composites.

However, alkalized bamboo fiber based composites shows superior micro-hardness properties as compared to untreated bamboo fiber based composites irrespective of CBPD content. The effect of alkalization and CBPD content on tensile strength of composites is shown in **Figure 1(c)**. It is seen that the tensile strength of the composite increases when filler content increases from 0 wt% to 10 wt% and decreases with further increase in filler content from 10 wt% to 20 wt%, in both treated and untreated composites. The reduction in tensile properties is explained as follows: under the action of a tensile force the filler matrix interface is vulnerable to debonding depending on interfacial bond strength and this may lead to a break in the composite [18,19]. However, the treated bamboo fiber based composites shows better tensile strength as compared to untreated one as expected. **Figure 1(d)** shows the variation of flexural strength of composites with CBPD content and alkalization of fibers.

The results exhibit similar trend as in the case of tensile test. It is interesting to note that addition of CBPD content (10 wt%) improves the flexural strength of the bamboo-epoxy composite. However, further addition (up to 20 wt%), lowers the strength in both the treated and untreated composites. There can be two reasons for this decline in the strength properties of these composites. One possibility is that the chemical reaction at the interface between the filler particles and the matrix may be too weak to transfer the stress; the other is that the corner points of the irregular shaped particulates result in stress concentration in the matrix [20]. It is also observed from the figure that there is significant improvement of flexural strength in case of alkalized fiber based composites as compared to untreated one. **Figure 1(e)** shows the effect of treatment and CBPD content on ILSS of composites. It is observed from the figure that the ILSS increases with increase in filler content in both treated and untreated composites. However treated fiber based composites shows better ILSS as compared to untreated fiber composites irrespective of filler content. In the present investigation, the span length is very short 40 mm. A large span to depth ratio in bending test increases the maximum normal stress without affecting the interlaminar shear stress, thereby increasing the tendency for longitudinal failure. If the span is short enough, failure initiates and propagates by interlaminar shear failure.

The maximum shear stress in a beam occurs at the midplane. So in the shear test, failure consists of a crack running along the midplane of the beam so that crack plane is parallel to the longitudinal plane. Effect of filler content and treatment on impact property of composites is shown in **Figure 1(f)**. It is observed that the impact strength of the composites is significantly improved by the addition of filler contents in case of treated composites. The increased filler content (up to 20 wt%) leads to a higher impact strength due to the interfacial reaction and provides an effective barrier for pinning and bifurcation of the advancing cracks. However, it shows opposite in case of untreated composites irrespective of filler content. The impact property of a material is its capacity to absorb and dissipate energies under impact or shock loading.

The impact performance of bamboo fiber-reinforced composites depends on many factors including the nature of the constituent, fiber/matrix interface and fiber/matrix/filler content, the construction and geometry of the composite and test conditions. The applied load transferred by shear to fibers may exceed the fiber/matrix interfacial bond strength to cause de-bonding. When the stress level exceeds the fiber strength, fiber fracture occurs. The fractured fibers may be pulled out of the matrix, which involves energy.

3.2. Steady State Erosion

3.2.1. Effect of Impact Velocity on Erosion Rate of the Composites

The velocity of the erosive particle has a very strong effect on the wear process. If the velocity is very low, then stresses at impact are insufficient for plastic deformation to occur and wear proceeds by surface fatigue [21]. When the velocity increases, the eroded material may deform plastically upon particle impact. In this regime, wear is caused by repetitive plastic deformation. At brittle wear response, proceeds by subsurface cracking. At very high particle velocities melting of the impacted surface may even occur. The variation of erosion rate with impact velocity is shown in **Figure 2(a)** for both the treated and untreated fiber based composites. Erosion trials are conducted at four different impact velocities under constant operating condition (impingement angle: 60˚, stand-off distance: 75mm, erodent size 250 μm). The figure shows that erosion rate of treated bamboo composites is less than that of the untreated bamboo composite. The erosion rate reaches its maximum at the impact velocity of 65 m/sec for both the treated and untreated fiber composites.

3.2.2. Effect of Impingement Angle on Erosion Rate of the Composites

Impingement angle is also an important parameter for the erosion process. It is defined as the angle between the target material and the trajectory of the erodent. Dependence of erosion rate on the impact angle is largely determined by the nature of the target material.

In the literature [22-25], materials are broadly classified as ductile or brittle, based on the dependence of their

erosion rate with impingement angle. The ductile behavior is characterized by maximum erosion rate at low impingement angle (typically ranges from 15˚ to 30˚). On the other hand, if the maximum erosion rate occurs at normal impact (90˚), the behavior of the material is brittle. Reinforced composites have been found to exhibit semi-ductile behavior with the maximum erosion rate at intermediate impingement angles (typically ranges from 45˚ to 60˚). **Figure 2(b)** shows the effect of impingent angle on erosion rate of composites under specified operating conditions (impact velocity: 45 m/sec, stand-off distance: 75 mm, erodent size: 250 μm). The figure shows that the peak of erosion rate occurs at an impingement angle of 45˚ for untreated bamboo composites, whereas for the treated bamboo composites the peak erosion rate is around 60˚ impingement angle. This clearly indicates that these composites respond to solid particle impact, neither in a purely ductile nor in a purely brittle manner. This behavior can be termed as semi-ductile in nature. Further it is also observed from the figure that the erosion rate of treated fiber composites shows less erosion rate as compared to untreated fiber composites irrespective of impingement angles.

3.3. Analysis of Experimental Results

The analysis has been carried out using the popular software MINITAB 15. **Table 2** shows the comparison of erosion rates between treated and untreated bamboo fiber based composites. In the table the seventh and the ninth columns represent S/N ratios of the erosion rates for untreated and treated bamboo based composites respectively. The overall mean for the S/N ratio of the erosion rate is found to be 61.80 db for the untreated samples and 62.21 db for treated ones. Analysis of the result leads to the conclusion that factor combination of A1, B3, C2, D1 and E3 gives minimum erosion rate for the untreated samples, whereas for the treated samples, the optimal combination of factor settings are A1, B2, C2, D1 and E2 respectively.

3.4. Surface Morphology of Eroded Surfaces

Figure 3 shows the SEM images of the untreated bamboo fiber based composites. From **Figure 3(a)** it is evident that the fibers are chipped off and broken, with impact angle of 30˚ and velocity of 45 m/sec with CBPD content of 0 wt%. **Figure 3(b)** shows the micrograph of eroded surface of 10 wt% of CBPD filled composite at an impact angle of 30˚ and the velocity of 45 m/s. It is evident from the micrographs that the hard erodent particles penetrate the surface and cause material removal mostly by micro-ploughing. When impingement angle is increased to 60˚, a relatively small fraction of the material is seen to be removed from the surface although formation of large amount of grooves is visible. However, the crack formation and propagation is not seen (**Figure 3(c)**), with further increase in impingement angle to 90˚. Micrograph shows the formation of larger craters due to the material loss and the arrays of broken and semi-broken fibers within. Due to the repeated impact of hard sand particles, there is initiation of cracks on the fibers and as erosion progresses, these cracks subsequently propagate on the fiber bodies both in transverse as well as longitudinal manner as shown in **Figure 3(d)**. Micrograph of the surface having 20 wt% CBPD eroded at an impingement angle of 60˚ and an impact velocity of 45 m/s is shown in **Figure 3(e)**.

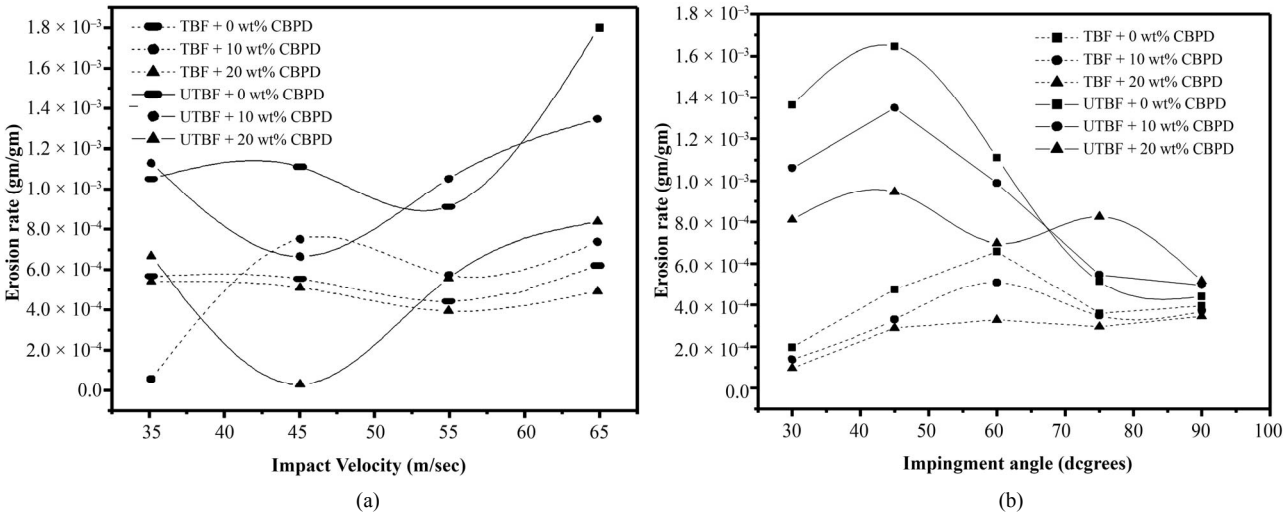

Figure 2. (a) Effect of impact velocity on erosion rate of the composites; (b) Effect of impingement angle on erosion rate of the composites.

Table 2. Comparison of erosion rates between CBPD filled treated and untreated bamboo epoxy composites as per L27 orthogonal array.

Expt. No.	A	B	C	D	E	Er (UT)	S/N (db)	Er (T)	S/N (db)
1	45	0	30	65	125	3.48E−05	89.17	3.33E−05	89.55
2	45	0	60	75	250	5.48E−04	65.22	5.24E−04	65.61
3	45	0	90	85	350	6.57E−04	63.65	6.28E−04	64.04
4	45	10	30	75	250	6.65E−04	63.54	6.36E−04	63.93
5	45	10	60	85	350	2.69E−04	71.41	2.57E−04	71.80
6	45	10	90	65	125	4.38E−05	87.17	4.19E−05	87.56
7	45	20	30	85	350	2.01E−04	73.94	1.92E−04	74.32
8	45	20	60	65	125	5.97E−05	84.48	5.71E−05	84.87
9	45	20	90	75	250	9.17E−03	40.74	8.77E−03	41.13
10	55	0	30	75	350	2.83E−03	50.96	2.71E−03	51.34
11	55	0	60	85	125	1.73E−03	55.21	1.66E−03	55.60
12	55	0	90	65	250	2.13E−03	53.43	2.04E−03	53.81
13	55	10	30	85	125	3.46E−02	29.22	3.31E−02	29.61
14	55	10	60	65	250	4.93E−04	66.13	4.72E−04	66.52
15	55	10	90	75	350	3.35E−04	69.50	3.20E−04	69.89
16	55	20	30	65	250	7.85E−04	62.10	7.51E−04	62.48
17	55	20	60	75	350	9.02E−04	60.89	8.63E−04	61.28
18	55	20	90	85	125	9.63E−04	60.33	9.21E−04	60.71
19	65	0	30	85	250	3.15E−03	50.02	3.02E−03	50.41
20	65	0	60	65	350	3.71E−03	48.60	3.55E−03	48.99
21	65	0	90	75	125	8.44E−04	61.47	7.40E−04	62.61
22	65	10	30	65	350	1.11E−03	59.07	1.06E−03	59.46
23	65	10	60	75	125	3.78E−03	48.45	3.61E−03	48.83
24	65	10	90	85	250	6.79E−04	63.36	6.50E−04	63.74
25	65	20	30	75	125	1.28E−02	37.86	1.22E−02	38.25
26	65	20	60	85	250	2.50E−05	92.05	2.39E−05	92.44
27	65	20	90	65	350	3.48E−05	89.17	8.90E−04	61.01

Note: UT: Untreated; T: Treated; Er(UT): Erosion rate of untreated bamboo fiber composites (gm/gm); Er(T): Erosion rate of treated bamboo fiber composites (gm/gm).

A small portion of a fiber exposed during the sand erosion is noticed. The matrix covering the fiber seems to be chipped off, and the crater thus formed shows the fiber body, which is almost intact. Repeated impact of the erodent has caused roughening of the surface. When the impact velocity is increased to 55 m/s, crater formation is observed due to penetration of hard silica sand particles onto the surface cause material removal mostly from the matrix regime. Small cracks and multiple fractures are also distinctly seen in this micrograph (**Figure 3(f)**). Particle impingement produces a rise in temperature of the surface, which makes the matrix deformation easy because the high temperature softens the matrix [23]. On impact, the erodent particle kinetic energy is transferred to the composite body that leads to crater formation and subsequently material loss. **Figure 3(g)** shows the surface of the 10 wt% of CBPD filled composite eroded at an impact angle of 60˚ and velocity of 65 m/sec. In this micrograph, the crack formation and propagation are clearly visible along with the groove formation, which implies the removal of the bulk mass of materials from the surface. When filler content is increased to 20 wt%,

micrograph shows the crater formation due to penetration of hard silica sand particles onto the surface and cause of material removal mostly from the matrix regime. Small cracks and multiple fractures are also distinctly shown in this micrograph (**Figure 3(h)**).

SEM images of the treated bamboo fiber based composites samples are shown in **Figure 4**. It is clear from the **Figure 4(a)** that the erosion rate is maximum in case of unfilled treated fiber composites. **Figure 4(b)** shows the plastic flow of matrix material along the erosion direction for the composite having 10 wt% CBPD eroded at lower impact angle (30˚). When impacting at such a low angle, the hard erodent particles penetrate the surface and cause material removal mostly by micro-ploughing. It is possible to investigate the particle flow direction easily from the wear trace on the matrix body. At 60˚ impact angle, micrograph (**Figure 4(c)**) shows that the

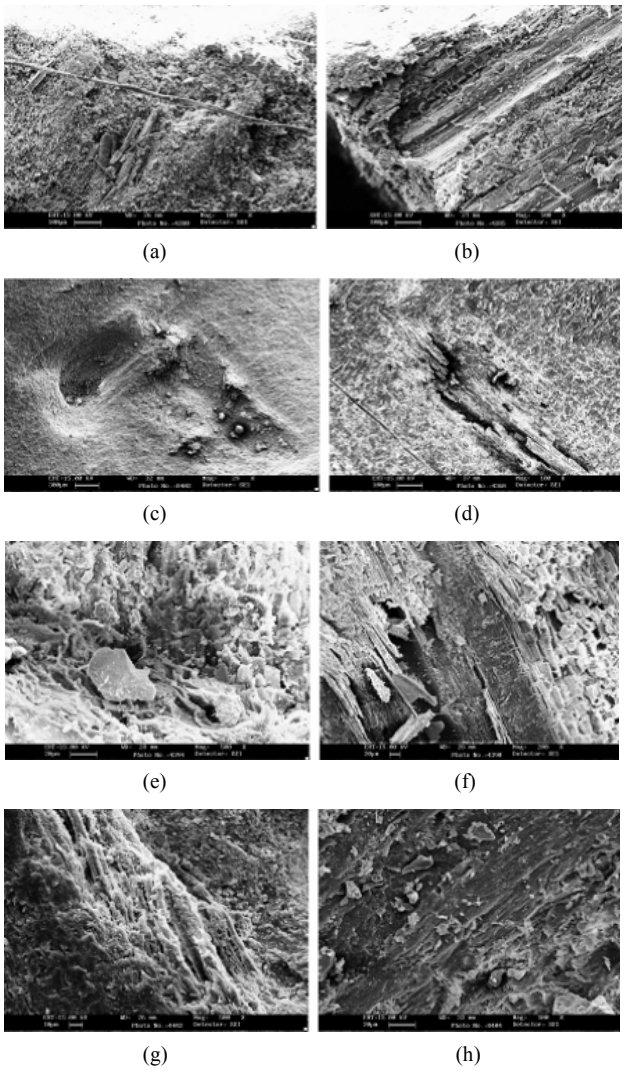

Figure 3. SEM images of eroded surfaces of untreated bamboo fiber composites.

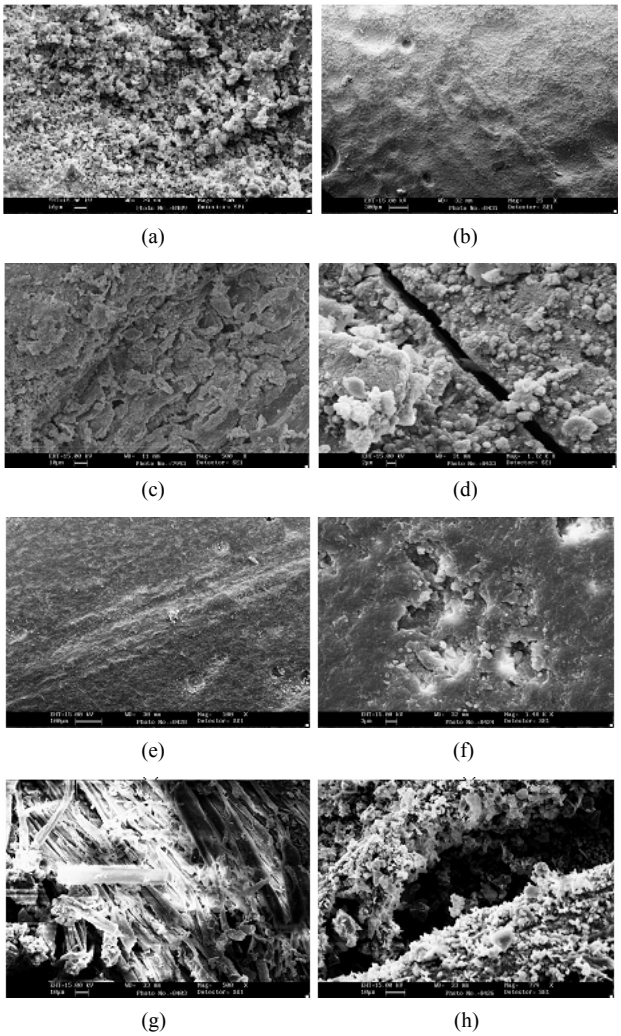

Figure 4. SEM images of eroded surfaces of treated bamboo fiber composites.

matrix is plastically deformed and amount of deformation is proportional to impact velocity of particles. At lower impact velocity, removal of matrix along the length of the fiber and subsequently exposed fiber getting removed and this can be seen from the micrograph.

Under normal impact, formation of micro-cracks and embedment of fragments of sand particles in composite is evident from the micrographs. During normal impact, the largest part of the initial energy is converted in to heat and hence matrix is softened which resulted in embedment of sand particles (**Figure 4(d)**). At an impact angle of 60˚, the fibers are chipped off due to the repeated impact of hard silica sand particles at impact angle (**Figure 4(e)**). A crater thus formed shows an array of almost intact fibers. After the local removal of matrix, this array of fibers is exposed to erosive environment. **Figure 4(f)** shows the micrograph of the surface having 20 wt% CBPD eroded at an impingement angle of 60˚

and an impact velocity of 55 m/s. The broken fiber and CBPD filler fragments are mixed with the matrix micro flake debris, and the damage of the composite is characterized by separation and detachment of this debris. Particle impingement produces a rise in temperature of the surface, which makes the matrix deformation easy. The higher impact speed of 65 m/s (**Figure 4(g)**) makes the sample surface remarkably rough as compared to the lower impact speed of 45 m/s. Subsequently the material removal becomes faster. The wear trace is distinctly visible and the protrusion of fibers beneath the matrix layer is seen. **Figure 4(h)** shows the large cracks on the surface. Crack formation and propagation is visible in micrographs.

3.5. ANOVA and the Effects of Factors

Analysis of Variance (ANOVA) is done from the experimental data for both treated and untreated bamboo fiber composites to determine the significant control factors and their effective interaction effect on erosion rate. **Tables 3(a)** and **(b)** show the ANOVA result for the erosion rate of untreated bamboo fiber and treated bamboo fiber based composites under solid particle erosion. This analysis was undertaken for a level of confidence of significance of 5%. From **Table 3(a)**, it has been observed that the impact velocity, stand-off distance, impingement angle and filler content have great influence on erosion wear rate.

The interaction of filler content and impingement angle shows significant contribution on the erosion rate and the rest factors and their interactions have comparatively less significant effect on erosion rate. Similarly from **Table 3(b)**, for treated bamboo fiber composites it is clear that the impact velocity, stand-off distance, impingement angle, filler content have great influence on erosion rate. The interaction of filler content and impingement angle shows significant contribution on the erosion rate but the remaining factor and interactions have relatively less significant contribution on erosion rate.

4. Conclusion

Successful fabrication of CBPD filled untreated and alkalized bamboo fiber reinforced epoxy composites have been developed by simple hand-lay-up techniques. It is observed from the study that there is a significant influence of CBPD content and treatment on physical mechanical behavior of composites. The mechanical properties of the treated bamboo fiber reinforced composites are found to be superior in comparison to those of untreated bamboo fiber composites. Also the use of alkalized bamboo fiber and incorporation of CBPD modifies

Table 3. (a) ANOVA for erosion rate of untreated bamboo fiber composites; (b) ANOVA for erosion rate of treated bamboo fiber composites.

(a)

Source	DF	Seq SS	Adj SS	Adj MS	F	P
A	2	1162.1	1162.1	581.0	2.50	0.143
B	2	69.5	69.5	34.8	0.15	0.863
C	2	328.4	328.4	164.2	0.71	0.522
D	2	699.7	699.7	349.9	1.21	0.389
E	2	1.6	1.6	0.8	0.00	0.997
A × B	4	292.6	292.6	73.2	0.31	0.860
A × C	4	636.2	636.2	159.1	0.68	0.622
B × C	4	1622.7	1622.7	405.7	1.75	0.233
Error	8	1859.5	1859.5	232.4		
Total	26	5971.0				

(b)

Source	DF	Seq SS	Adj SS	Adj MS	F	P
A	2	1156.3	1156.3	578.1	1.97	0.254
B	2	66.6	66.6	33.3	0.11	0.896
C	2	329.1	329.1	164.6	0.56	0.610
D	2	690.2	690.2	345.1	1.17	0.397
E	2	1.2	1.2	0.6	0.00	0.998
A × B	4	292.6	292.6	73.2	0.31	0.860
A × C	4	636.2	636.2	159.1	0.68	0.622
B × C	4	1622.7	1622.7	405.7	1.75	0.233
Error	8	1859.5	1859.5	232.4		
Total	26	5971.0				

Seq SS: Sequential sum of squares; Adj SS: Adjusted sum of squares; Adj MS: Adjusted mean of squares; F: Fishers Test; P: Statistical probability.

the erosion characteristics of the resulting composites. The peak erosion rate has been observed at 45˚ impingement angle for untreated bamboo-epoxy composites whereas, for treated bamboo-epoxy composites the peak erosion rate is found to be around 60˚ impingement angle. This result reveals the semi ductile nature of composites. From ANOVA analysis it has been observed that factors like impact velocity, stand-off distance, impingement angle and filler content have great influence on erosion wear rate for both untreated and treated bamboo fiber composites. However, the remaining factors have relatively less significant contribution on erosion rate. SEM studies of worn surfaces support the involved mechanisms and indicate plastic deformation, microcracking, melting, sand particle embedment, exposure of fibers and fiber-cracking etc. as the possibly occurring

phenomena behind material loss.

REFERENCES

[1] E. Bisanda and M. Ansell, "Properties of Sisal-CNSL Composites," *Journal of Materials Science*, Vol. 27, No. 6, 1992, pp. 1690-1700. doi:10.1007/BF00542934

[2] M. S. Sreekala, M. G. Kumaran and S. Thomas, "Oil Palm Fibers: Morphology, Chemical Composition, Surface Modification, and Mechanical Properties," *Journal of Applied Polymer Science*, Vol. 66, No. 5, 1997, pp. 821-835. doi:10.1002/(SICI)1097-4628(19971031)66:5<821::AID-APP2>3.0.CO;2-X

[3] V. G. Geethamma, R. Joseph and S. Thomas, "Short Coir Fiber-Reinforced Natural Rubber Composites: Effects of Fiber Length, Orientation, and Alkali Treatment," *Journal of Applied Polymer Science*, Vol. 55, No. 4, 1995, pp. 583-594. doi:10.1002/app.1995.070550405

[4] L. Mwaikambo and M. Ansell, "Chemical Modification of Hemp, Sisal, Jute and Kapok Fibres by Alkalization," *Journal of Applied Polymer Science*, Vol. 84, No. 12, 2002, pp. 2222-2234. doi:10.1002/app.10460

[5] A. Satapathy and A. Patnaik, "Analysis of Dry Sliding Wear Behavior of Red Mud Filled Polyester Composites Using the Taguchi Method," *Journal of Reinforced Plastics and Composites*, Vol. 29, No. 19, 2010, pp. 2883-2897. doi:10.1177/0731684408092453

[6] B. Pukanszky, "Particulate Filled Polypropylene: Structure and Properties," In: J. Karger-Kocsis, Ed., *Polypropylene*: *Structure*, *Blends* and *Composites*, Chapman and Hall, London, 1995, pp. 1-70. doi:10.1177/0731684408092453

[7] J. L. Acosta, E. Morales, M. C. Ojeda and A. Linares, "Effect of Addition of Sepiolite on the Mechanical Properties of Glass Fiber Reinforced Polypropylene," *Die Angewandte Makromolekulare Chemie*, Vol. 138, No. 1, 1986, pp. 103-110. doi:10.1002/apmc.1986.051380108

[8] R. N. Rothon, "Mineral Fillers in Thermoplastics: Filler Manufacture," *Journal Adhesion*, Vol. 64, No. 1, 1997, pp. 87-109.

[9] R. N. Rothon, "Mineral Fillers in Thermoplastics: Filler Manufacture and Characterization," *Advances in Polymer Science*, Vol. 139, 1999, pp. 67-107. doi:10.1007/3-540-69220-7_2

[10] B. Z. Jang, "Advanced Polymer Composites: Principles and Applications," CRC Press, Boca Raton, 1994, p. 52.

[11] S. W. Gregory, K. D. Freudenberg, P. Bhimaraj and L. S. Schadler, "A Study on the Friction and Wear Behavior of PTFE Filled with Alumina Nanoparticles," *Wear*, Vol. 254, No. 5-6, 2003, pp. 573-580. doi:10.1016/S0043-1648(03)00252-7

[12] K. Jungil, P. H. Kang and Y. C. Nho, "Positive Temperature Coefficient Behavior of Polymer Composites Having a High Melting Temperature," *Journal of Applied Polymer Science*, Vol. 92, No. 1, 2004, pp. 394-401. doi:10.1016/S0043-1648(03)00252-7

[13] B. D. Agarwal and L. J. Broutman, "Analysis and Performance of Fiber Composites," 2nd Edition, John Wiley and Sons, Inc., Hoboken, 1990.

[14] A. W. Ruff and L. K. Ives, "Measurement of Solid Particle Velocity in Erosive Wear," *Wear*, Vol. 35, No. 1, 1975, pp. 195-199. doi:10.1016/0043-1648(75)90154-4

[15] R. Zhou, D. H. Lu, Y. H. Jiang and Q. N. Li, "Mechanical Properties and Erosion Wear Resistance of Polyurethane Matrix Composites," *Wear*, Vol. 259, No. 1-6, 2005, pp. 676-683. doi:10.1016/j.wear.2005.02.118

[16] S. Biswas and A. Satapathy, "A Comparative Study on Erosion Characteristics of Red Mud Filled Bamboo-Epoxy and Glass-Epoxy Composites," *Materials and Design*, Vol. 31, No. 4, 2010, pp. 1752-1767. doi:10.1016/j.matdes.2009.11.021

[17] A. Satapathy, A. K. Jha, S. Mantry, S. K. Singh and A. Patnaik, "Processing and Characterization of Jute-Epoxy Composites Reinforced with SiC Derived from Rice Husk," *Journal of Reinforced Plastics and Composites*, Vol. 29, No. 18, 2010, pp. 2869-2878.

[18] A. Satapathy, A. Patnaik and M. K. Pradhan, "A Study on Processing, Characterization and Erosion Behavior of Fish (Labeo-Rohita) Scale Filled Epoxy Matrix Composites," *Materials and Design*, Vol. 30, No. 7, 2009, pp. 2359-2371. doi:10.1016/j.matdes.2008.10.033

[19] A. Patnaik, A. Satapathy, S. S. Mahapatra and R. R. Dash, "Modified Erosion Wear Characteristics of Glass-Polyester Composites by Silicon Carbide Filling: A Parametric Study Using Taguchi Technique," *International Journal of Materials and Product Technology* (*IJMPT*), Vol. 38, No. 2-3, 2010, pp. 131-152. doi:10.1016/j.matdes.2008.10.033

[20] A. Patnaik, A. Satapathy, S. S. Mahapatra and R. R. Dash, "A Comparative Study on Different Ceramic Fillers Affecting Mechanical Properties of Glass-Polyester Composites," *Journal of Reinforced Plastics and Composites*, Vol. 28, No. 11, 2009, pp. 1305-1318. doi:10.1177/0731684407086589

[21] G. W. Stachowiak and W. Batchelor, "Engineering Tribology, Series 24," Elsevier, Amsterdam, 1993, p. 586.

[22] S. M. Kulkarani and K. Kishore, "Influence of Matrix Modification on the Solid Particle Erosion of Glass/Epoxy Composites," *Polymer Composites*, Vol. 9, No. 1, 2001, pp. 25-30.

[23] J. Zahavi and G. F. Schmitt, "Solid Particle Erosion of Reinforced Composite Materials," *Wear*, Vol. 71, No. 2, 1981, pp. 179-190. doi:10.1016/0043-1648(81)90337-9

[24] U. S. Tewari, A. P. Harsha, A. M. Hager and K. Friedrich, "Solid Particle Erosion of Unidirectional Carbon Fiber Reinforced Polyetheretherketone Composites," *Wear*, Vol. 252, No. 11-12, 2002, pp. 992-1000.

[25] U. S. Tewari, A. P. Harsha, A. M. Hager and K. Friedrich, "Solid Particle Erosion of Carbon Fibre- and Glass Fibre-Epoxy Composites," *Composites Science and Technology*, Vol. 63, No. 3, 2003, pp. 549-557.

